



Analytical Expressions and Interpolations for Coil Spring Experimental Data

Franz Biehl
August 4, 1997

Abstract

Analytical expressions and interpolation curves for storage and loss modulus in the frequency domain are obtained for several coil spring configurations. These configurations consist of a damped coil on epoxy seats, a damped coil on Fluorel viscoelastic seats, and an undamped coil on Fluorel seats. The reported results are used in an analytical spring stack model to predict the complex eigenvalues and frequency response transfer functions. Comparison of test data with an analytical model is favorable.

Table of Contents

| | |
|---|-----------|
| 1. Problem Description | 3 |
| 2. Coil Spring Assembly Configurations | 3 |
| 3. Fit Expressions and Discreet Interpolation Values | 3 |
| 3.1 General Procedure | 3 |
| 3.2 Fluorel Seat Stiffness and Loss Factor | 4 |
| 3.2.1 General Approach | 4 |
| 3.2.2 Fluorel Stiffness Material Modulus..... | 4 |
| 3.2.3 Complex Stiffness of Damped Coil on Epoxy Seats | 4 |
| 3.2.4 Complex Stiffness of Damped Coil on Fluorel Seats | 4 |
| 3.2.5 Complex Stiffness on Fluorel Seats..... | 5 |
| 3.3 Damped Coil on Epoxy | 6 |
| 3.4 Undamped Coil on Fluorel Seats | 7 |
| 3.5 Damped Coil on Fluorel Seats Modulus | 8 |
| 4. Comparison of Analytical Model with Test Data | 9 |
| 5. Conclusions | 10 |
| 6. References | 11 |

1. Problem Description

The purpose of this work is to extend measured experimental spring data results over a broader frequency range for subsequent simulation of the LIGO spring stack assembly. Experimental data are fitted with analytical functions or interpolation curves in the frequency domain for coil spring storage and loss modulus. Data are derived for both axial and shear directions.

2. Coil Spring Assembly Configurations

Frequency dependent storage modulus or stiffness (K) and loss factors (h) are generated for three spring configurations described as 1) damped coil on epoxy, 2) undamped coil on Fluorel, and 3) damped coil on Fluorel. Figure 1 shows a schematic of a coil spring assembly and defines the axial and shear directions.

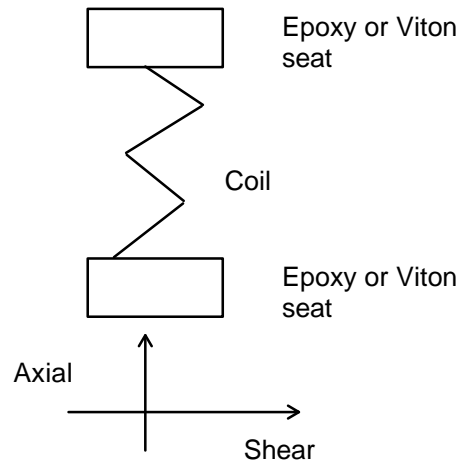


Figure 1: Test Coil Spring Assembly

Tabulated test results in a frequency range from about 0.5 Hz to 2 Hz for the three configurations are presented in Reference 1. Static spring rates are obtained from static load versus deflection curves found in [4]. These data form the set of experimental values used in to generate spring models.

3. Fit Expressions and Discreet Interpolation Values

3.1 General Procedure

In general, exponential functions are used to fit experimental stiffness data whereas linear piece wise interpolation is used for loss factor data. Experimental data are first fitted with a curve from zero to 2.2 Hz for interpolation at a common set of frequencies so that comparisons can be obtained between axial and shear results for the same configuration and also between different configurations. Where available, zero frequency stiffness values

are obtained from measured data or from analytical models. For example, the ratio of shear to axial stiffness at a set of common frequencies is averaged to define a ratio to be used for static shear stiffness when an experimental value for the static axial stiffness is known. In all cases the loss factor at zero frequency is set to zero.

Results are tabulated in arrays of interpolated and/or extrapolated values as a function of discrete frequencies. These frequencies begin at zero and increment by 0.2 Hz up to and including 2.2 Hz and then are spread out in an increasing increment up to 1000 Hz for a total of 24 discrete values. An output array generated for each configuration is subsequently read into the stack simulation MATLAB program^[2] that computes stack resonant frequencies and frequency response functions.

3.2 Fluorel Seat Stiffness and Loss Factor

3.2.1 General Approach

The approach to obtaining the Fluorel seat stiffness and loss factor as functions of frequency is to subtract the damped coil complex modulus from the damped coil on Fluorel seats complex modulus at identical frequencies. A normalized curve of Fluorel material complex modulus test data is then applied to the calculated Fluorel seat modulus to extend the seat modulus over a larger frequency range.

3.2.2 Fluorel Stiffness Material Modulus

Fluorel polymer data^[3] give stiffness and loss factor at frequencies up to 1000 Hz. Stiffness data at all frequencies is normalized to unity at zero frequency and the loss factor is interpolated at values corresponding to the output frequency array. The normalized least squares fit to the stiffness is given by

$$K_{vit}(f) = -3.854e^{0.006f} + 4.843 \quad (1)$$

where K_{vit} is the stiffness in N/m and f is frequency in Hz.

3.2.3 Complex Stiffness of Damped Coil on Epoxy Seats

The complex stiffness of a damped coil is essentially equivalent to the complex stiffness of a damped coil on epoxy because the epoxy is rigid in both axial and shear directions. Stiffness and loss factor at five experimental frequencies plus zero frequency values are piecewise linearly interpolated at the set of discrete frequencies defined in Section 3.1 (this interpolation procedure is used for all the configurations discussed in the following sections). The axial static stiffness is 42,921 N/m^[4], while the zero frequency loss factor is set to zero. An averaged ratio of shear to axial stiffness is calculated from the data (average ratio = 1.856). That ratio is then used to generate a static shear stiffness value from the measured static axial stiffness.

3.2.4 Complex Stiffness of Damped Coil on Fluorel Seats

The static axial stiffness value is 39,695 N/m^[4] calculated from a straight line slope of force versus deflection. As in the previous section, the static shear stiffness is calculated from the average shear to axial stiffness ratio (shear to axial stiffness of damped coil on Fluorel seats = 1.38). Loss factor in both the axial and shear direction are obtained at the desired interpolated frequencies that include the zero loss factor at zero frequency.

3.2.5 Complex Stiffness on Fluorel Seats

Complex stiffness of Fluorel seats is calculated as the difference between the complex stiffness of the damped coil on Fluorel and the damped coil on epoxy. Complex stiffnesses in series add as reciprocals, thus

$$\bar{K}_{fl}(f) = \frac{2}{\left[\frac{1}{\bar{K}_{dv}(f)} - \frac{1}{\bar{K}_{de}(f)} \right]} \quad (2)$$

where \bar{K} denotes complex stiffness and the subscripts fl , dv , and de are Fluorel seat, damped coil on Fluorel, and damped coil on epoxy. The 2 is required because there are two Fluorel seats as indicated in Figure 1. The Fluorel seat stiffness is the real part of \bar{K}_{vit} while the loss factor is the imaginary part of \bar{K}_{vit} divided by the real part of \bar{K}_{vit} .

An averaged ratio of the calculated Fluorel seat stiffness (from equation 2) to the normalized Fluorel material stiffness (from equation 1) is applied to the material stiffness curve to generate the Fluorel seat stiffness up to 1000 Hz (axial and shear). Fluorel seat loss factor in both axial and shear directions is the same as the Fluorel material loss factor because material loss factors are independent of structural arrangements. Loss modulus, however, is the product of storage modulus and loss factor at a given frequency and thus differs as a result of the shape and size of the damping material object.

Figure 2 displays the Fluorel seat calculated axial and shear stiffness in the frequency range from 0 to 1000 Hz. Note that the axial stiffness is greater than the shear stiffness as would be expected for a rubber-like material whose shear dimension (seat diameter) is about 4 times the axial dimension (seat height). The interpolated loss factor for Fluorel material appears in Figure 3.

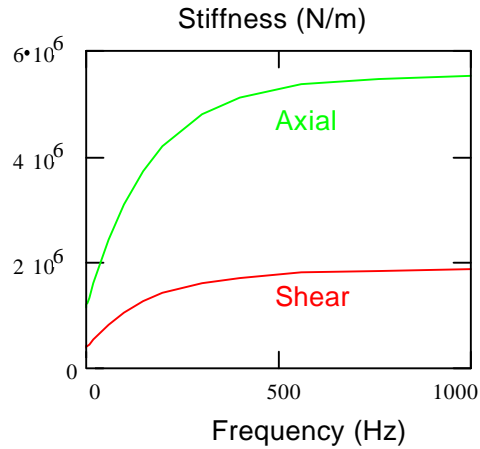


Figure 2: Fluorel stiffness in axial and shear directions as a function of frequency.

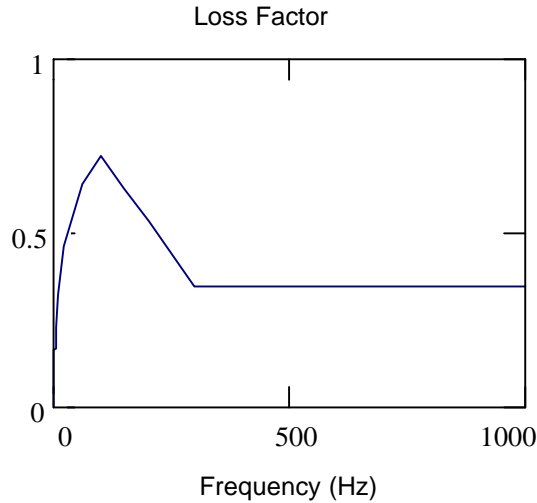


Figure 3: Fluorel material loss factor as a function of frequency.

3.3 Damped Coil on Epoxy

Axial stiffness for the damped coil on epoxy is generated using the test data values plus the zero frequency value (42,921 N/m) and a value at 1000 Hz of 47,210 N/m^[5]. The least squares curve fit for these data is given by

$$K_{de}(f) = -5422 e^{-2.77f} + 48330. \quad (3)$$

Shear stiffness for the damped coil on epoxy is generated using the shear to axial ratio derived in section 3.2.3. Axial and shear loss factor curves are generated using the test data plus values for 0 and 1000 Hz. Loss factors above 5 Hz are assumed equal to 0.024 in the axial direction and 0.016 in the shear direction. Figures 4 and 5 show the resulting curves plus test data (circles) up to 5 Hz.

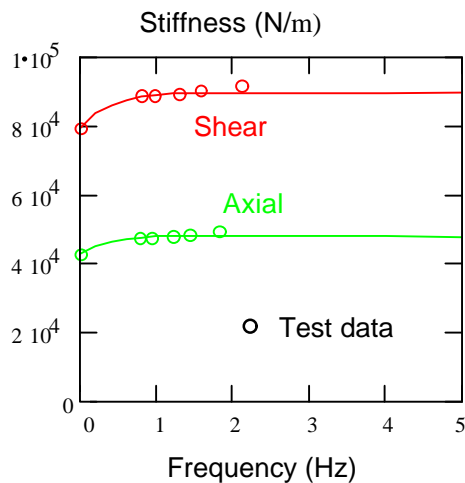


Figure 4: Damped coil on epoxy axial and shear stiffness as a function of frequency.

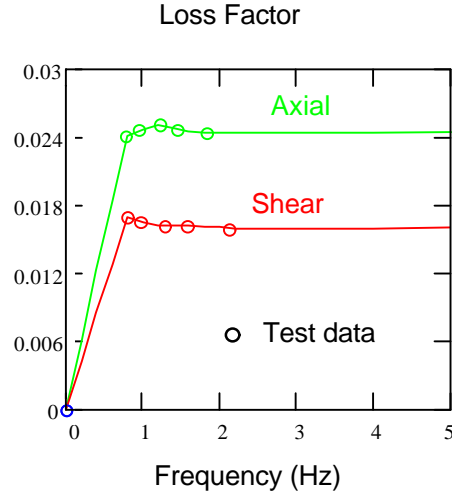


Figure 5: Damped coil on epoxy axial and shear loss factor as a function of frequency.

3.4 Undamped Coil on Fluorel Seats

Curves for the undamped coil on Fluorel are generated by a sum of complex stiffness of the coil and two Fluorel seats expressed by

$$\bar{K}_{uf}(f) = \frac{1}{\left[\frac{2}{K_{fl}(f)[1+h_{fl}(f)]} + \frac{1}{K_{de}} \right]}, \quad (4)$$

where the subscripts *uf*, *fl*, and *de* denote undamped coil on Fluorel, Fluorel, and static stiffness of damped coil on epoxy; respectively. The undamped complex stiffness is calculated at the output array frequencies for both axial and shear directions. As indicated previously, stiffness is equal to the real part of $\bar{K}_{fl}(f)$ and loss factor to the ratio of the imaginary part to the real part of $\bar{K}_{uf}(f)$. Figures 6 and 7 summarize the results for the undamped coil on Fluorel seats.

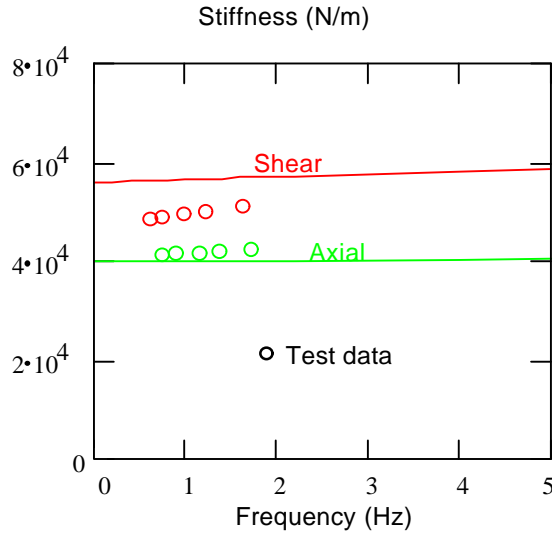


Figure 6: Undamped coil on Fluorel seats axial and shear stiffness as a function of frequency.

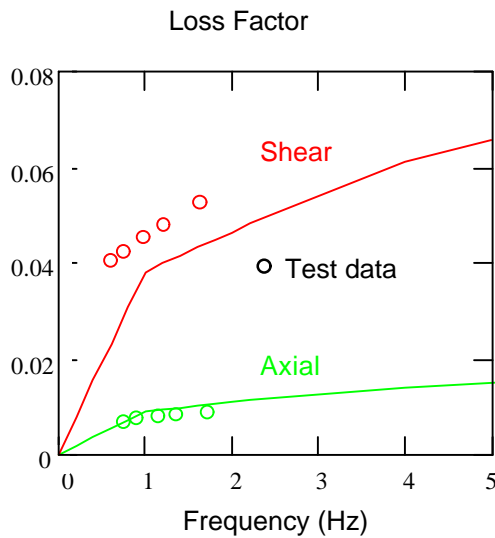


Figure 7: Undamped coil on Fluorel seats loss factor as a function of frequency.

An examination of Figures 6 and 7 reveals that the test data fit the constructed curves better in the shear direction than in the axial direction; although both show reasonable agreement. This suggests that the model for the Fluorel seats developed in Section 3.2 using Fluorel material properties shown in Figures 2 and 3 is acceptable.

3.5 Damped Coil on Fluorel Seats Modulus

Damped coil on Fluorel seat curves are generated by an equation similar to Equation 4 except that the coil stiffness at zero frequency is replaced by the damped coil complex modulus at each desired frequency.

$$\bar{K}_{df}(f) = \frac{I}{\left[\frac{2}{K_{fl}(f)[1 + jh_{fl}(f)]} + \frac{I}{K_{de}(f)[1 + jh_{de}(f)]} \right]}, \quad (5)$$

where the stiffness and loss factor are calculated from the real and imaginary parts of the complex stiffness $\bar{K}_{df}(f)$. Figures 8 and 9 display the results for the damped coil on Fluorel.

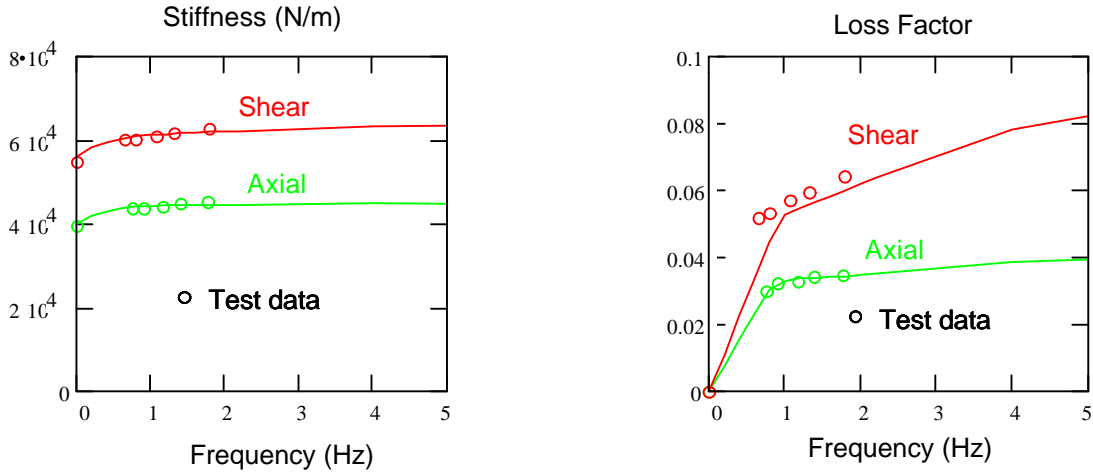


Figure 8: Damped coil on Fluorel seats stiffness and loss factor as a function of frequency.

As would be expected, the test data points are nearly coincident with the calculated curves because the complex modulus is constructed from extracted test data Fluorel seat modulus and from extracted test data damped coil modulus.

4. Comparison of Analytical Model with Test Data

A comparison of an theoretical coil model with test data for a damped coil on epoxy is presented in this section. Derivation of the analytical model is discussed in Reference 5 while a procedure for correcting the calculated model results for a variation in the assumed damping material temperature is presented in Reference 6. A temperature correction from the published damping material temperature (77⁰ F) to the expected test temperature (assumed 72⁰ F) is used in the theoretical model. The results are shown in Figures 10 and 11 where the solid lines denote theoretical model results and the circles test data.

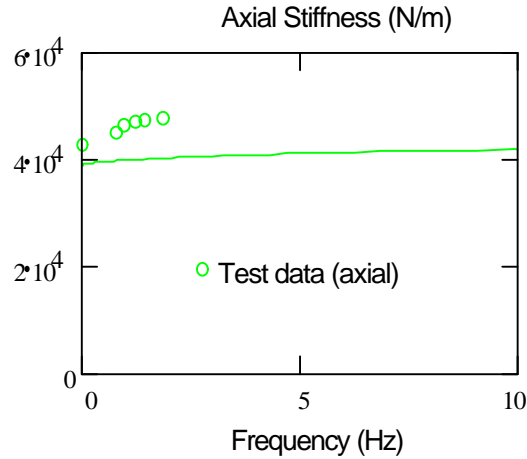


Figure 10: Damped coil on epoxy comparison of theoretical model axial stiffness with test data

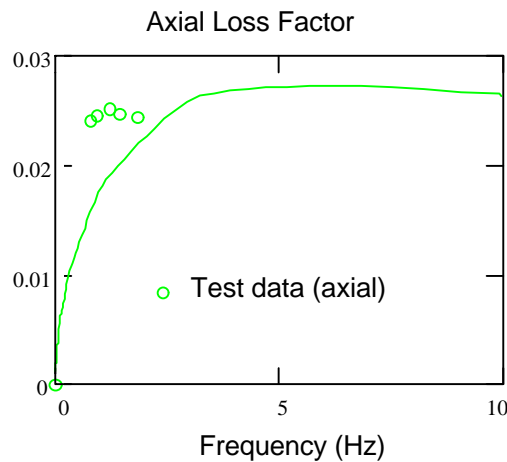


Figure 11: Damped coil on epoxy comparison of theoretical model axial loss factor with test data

Theoretical model calculated results are strongly influenced by very small variations in the spring geometric dimensions (wall thickness, diameter, effective length), end friction factors, and damping material distributions. It is, therefore, not unexpected to see some variation between the calculated and test results as shown in Figures 10 and 11.

5. Conclusions

This Technical Note describes the preparation of LIGO coil spring stiffness and loss factor data to be used in subsequent spring stack analytical models. A combination of test data and damping material characteristics are employed to develop the frequency dependent stiffness and loss factor values. The test data and fitted analytical curves appear to conform to expected behavior.

6. References

1. E. Ponslet, *Low Frequency Damping Measurement Setup and First Results*, HYTEC Inc., LIGO document HYTEC-TN-LIGO-17, June 1997
2. E. Ponslet, *Isolation Stack Modeling*, HYTEC Inc., Los Alamos, NM, document HYTEC-TN-LIGO-01, January 23, 1996.
3. Email communication 18 December 1995 from Joseph Giaime
4. Eric Ponslet, *LIGO Coil Springs Test Report*, HYTEC Inc., LIGO document HYTEC-TN-LIGO-14, February, 1997
5. E. Ponslet, *Design of Vacuum Compatible Damped Metal Springs for Passive Isolation of The LIGO Detectors*, HYTEC Inc., Los Alamos, NM, document HYTEC-TN-LIGO-04a (revision a), January 1997.
6. F. Biehl, *Temperature Effects on LIGO Damped Coil Spring*, HYTEC Inc., Los Alamos, NM, document HYTEC-TN-LIGO-18, May 1997.

Note 1, Linda Turner, 09/03/99 02:09:43 PM
LIGO-T970242-00-D